

Heterohexacene Diimides: *Anti*- and *Syn*- Isomers and Quinonoid Forms

Kang Cai, Jiajun Xie, Xiao Yang, and Dahui Zhao*

Beijing National Laboratory for Molecular Sciences, Department of Applied Chemistry and the Key Laboratory of Polymer Chemistry and Physics of the Ministry of Education, College of Chemistry, Peking University, Beijing, China

S Supporting Information

ABSTRACT: A number of *anti*- and *syn*- isomers of heterocyclic hexacene diimides containing NH and O/S are synthesized. Two stable quinonoid diimides displaying low LUMO levels at less than -4.1 eV are obtained via oxidation of the *anti*- isomers. Reducing the isolated quinonoid molecules back to dihydro- forms offer pure *anti*- isomers.



Naphthalene tetracarboxylic diimide and derivatives (NDIs) have recently attracted great attention for their desirable electronic properties.^{1,2} Particularly, with 2,6-dibromo- and 2,3,6,7-tetrabromo-1,4,5,8-naphthalene diimides (2Br-NDI³ and 4Br-NDI⁴) as efficient synthons, various extended acenes and heteroacenes with dicarboximide functionality⁵ are readily prepared as novel functional π -systems. For instance, dithiophene,⁶ diindole,⁷ and dithiozole-annulated⁸ NDIs exhibited ambipolar or n-type semiconductive properties, and tetraacene diimides manifested near-infrared (NIR) optical activities.⁹ N-Heteroacene diimides demonstrated distinctive self-assembly abilities and formed unique supramolecular nanostructures.^{10,11}

Previously, we reported a series of N-heterocyclic hexa- and heptacene dicarboximide molecules, which displayed appealing optical properties and self-assembling behaviors.¹² Among them, a dihydrotetraaza derivative 2H-TAHDl (Figure 1)

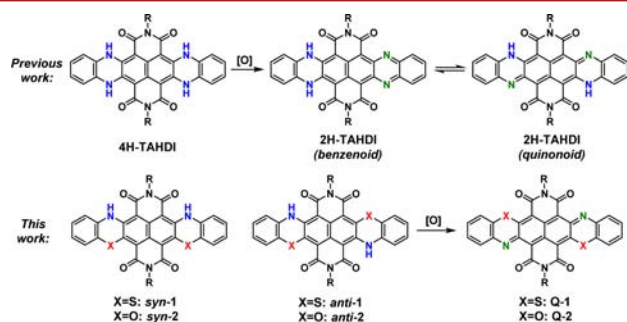


Figure 1. Structures of heterohexacene diimides.

uniquely underwent tautomerization between benzenoid and quinonoid forms.^{12a} Polycyclic π -systems with quinonoid structures are of particular interest for possessing distinct optical and electronic features from their benzenoid counterparts.¹³ Appropriate quinonoid polycyclic molecules were shown to possess open-shell ground state characteristics and exhibited special nonlinear optical and magnetic properties.^{13b-e}

Quinonoid heteropentacenes with low LUMO levels were demonstrated with notable electron-transporting capabilities.¹⁴ A unique feature of our previously investigated azaacene diimide was that its quinonoid form was of impressive stability, comparable to that of the benzenoid tautomer. However, the existence of this tautomerization equilibrium was inconvenient for utilization of the quinonoid structure. To circumvent this problem, we speculated replacing the two NH moieties with O or S atoms, which would offer fixed quinonoid molecules.

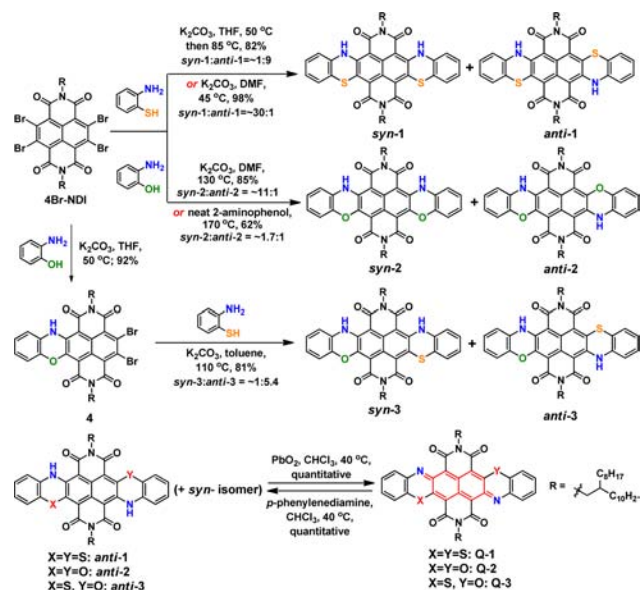
Accordingly, we designed a series of heterocyclic hexacene diimides containing N, S, and/or O atoms, which were all isoelectronic π -systems of 2H-TAHDl (Figure 1). Using our previously developed methodology, these new molecules ought to be attainable by oxidizing respective dihydro- precursors, which could be synthesized from 4Br-NDI upon condensation with 2-aminothiophenol or 2-aminophenol. A potential problem with this synthetic route was that two different regioisomers (*anti*- and *syn*-) were possibly formed but only the *anti*- isomers could be oxidized into the quinonoid products (Scheme 1).

We first conducted the condensation between 4Br-NDI and 2-aminothiophenol. When the reaction was carried out at elevated temperature in THF, some green solid was generated. High-resolution mass spectroscopy (HRMS) and elemental analysis (EA) both validated its chemical formula consistent with 1. Although only one spot was detected on thin layer chromatography (TLC), ¹H NMR revealed evidence for a regioisomer mixture. Two different resonances with an integral ratio of $\sim 1:9$ were observed between 12.4 and 12.8 ppm, assignable to the NH protons in different regioisomers. Furthermore, when this reaction product was treated with PbO₂ at 40 °C, most of it was converted into a blue compound showing a larger *R_f* value than that of the reactant on TLC, while a small amount of the original green material remained unchanged. ¹H/¹³C NMR, HRMS, and EA all confirmed that

Received: January 13, 2014

Published: March 14, 2014

Scheme 1. Synthetic Routes



the blue product was quinoidal **Q-1**. Based on these results, the major component of the green mixture was identified to be **anti-1**, and the minor product was **syn-1** (Scheme 1). The relative ratio of these two isomers was sensitively influenced by the condensation conditions. When the reaction was performed in DMF at 45 °C, **syn-1** became the dominant product, coexisting with ~3% **anti-1**. Oxidation of this mixture mostly containing **syn-1** with PbO_2 resulted in recovering most of the starting material after heating at an even higher temperature than 40 °C.

The selectivity for *syn*/*anti* was lowered at increased reaction temperature. When the reaction was conducted at 90 °C in DMF, the ratio of **syn-1**/**anti-1** dropped to ~1.5:1. Switching to other solvents also led to lowered selectivity (**syn-1**:**anti-1** = ~1:2.3 in $CHCl_3$ at 60 °C and ~1:1.8 in toluene at 110 °C). We deemed the reason for such varied regioselectivity in different solvents was complicated and involved a number of factors such as N vs S nucleophilicity changes with solvent, solvent polarity variance, hydrogen bonding, etc.

By comparing the 1H NMR spectra, **syn-1** and **anti-1** were found to have nearly identical aromatic resonances,¹⁵ but the NH chemical shifts were distinguishable (Figure 2). Additional discrepancy was depicted by α -protons on *N*-alkyl chains

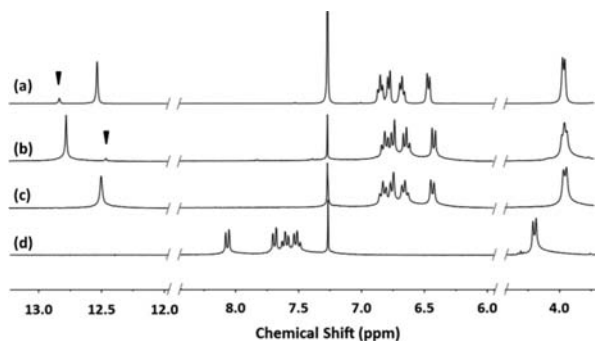


Figure 2. 1H NMR spectra of isomer mixture of **1** obtained from THF (a) and DMF (b) reaction solutions (triangles indicate the NH signal of minor product),¹⁵ pure **anti-1** (c, from reduction of **Q-1**), and **Q-1** (d).

(NCH_2).¹⁶ The two side groups on the imide nitrogen were identical in **anti-1**, whereas those in **syn-1** were chemically nonequivalent. Such differences were discerned by the 1H NMR, by showing the different resonance patterns of NCH_2 (Figure 2). This evidence further substantiated our structural assignments.¹⁷

Quinoidal **Q-1** was adequately stable in the solid state, and the 1H NMR spectrum of its $CDCl_3$ solution remained unchanged after a week under ambient conditions. However, this molecule was partially transformed back to **anti-1** when eluted from silica gel column chromatography. Apparently, the diimide groups rendered **Q-1** highly electron-deficient and easily reduced to **anti-1** with one more Clar sextet.¹³ Employing *p*-phenylenediamine as the reducing reagent allowed quantitative conversion of **Q-1** to **anti-1** at 40 °C in $CHCl_3$ to be realized.

The condensation of 2-aminophenol with **4Br-NDI** required a much higher temperature (130 °C) in DMF than its thioanalogue, likely due to the lower nucleophilicity of O than S. The resultant blue product was found to be almost completely **syn-2**, as evidenced by the NH and NCH_2 signals in the 1H NMR spectrum (see the Supporting Information). Nevertheless, a low-intensity resonance assignable to **anti-2** (~5%) was detected near the main NH signal. Changing the reaction solvent to *N*-methylpyrrolidone, THF, or toluene did not help increase the **anti-2**/**syn-2** ratio. Finally, heating **4Br-NDI** in neat 2-aminophenol at 170 °C yielded a mixture comprising **syn-2**/**anti-2** at ~1.7:1. The higher *syn*-selectivity observed with **2** in varied solvents was understandable. The stronger electron-donating ability and higher nucleophilicity of N compared to O favored the NH substitution of bromine *syn*-to the first nitrogen substitution.¹⁶

Oxidizing this 1.7:1 isomer mixture of **2** resulted in its partial conversion to a new blue compound. For an unknown reason, the unreacted residue retained a small amount of **anti-2** (**anti**/**syn** = ~1:10). The oxidation product **Q-2** was isolated. NMR and HRMS both verified its dehydro- identity. **Q-2** was also prone to reduction when exposed to silica gel, but it was fairly stable in the solid state, as no decomposition was detected by 1H NMR after storing under ambient conditions for over four months. Again, pure **anti-2** could be obtained by reduction of **Q-2** with *p*-phenylenediamine in quantitative yield.

We also endeavored to synthesize the asymmetric quinoidal **Q-3** (Scheme 1). A reaction between **4Br-NDI** and 2-aminophenol at 50 °C in THF offered 1:1 condensation product **4** in 92% yield. A further condensation of **4** with 2-aminothiophenol offered a mixture of **anti-3** and **syn-3**. After screening different solvents, the highest **anti**/**syn** ratio at ~5.4:1 was achieved in toluene. Upon oxidizing this isomer mixture with PbO_2 , the 1H NMR spectrum indicated that the major component of the resultant material was the desired product **Q-3**. However, **Q-3** was much more sensitive to silica gel than **Q-1** and **Q-2**. It quickly decomposed into unknown substances during column chromatography and could not be isolated or purified.

Thus, pure **anti-1**, **anti-2**, **Q-1**, and **Q-2** were obtained and applied to the following characterizations. Because of the nearly identical R_f values of regioisomer pairs on TLC, pure compounds of **syn-1**, **syn-2**, and **anti-3** were not attainable. Samples contaminated with a small amount of regioisomers were employed for characterizations (**syn-1** with ~3% **anti-1**, **syn-2** with ~5% **anti-2**, and **anti-3** with ~16% **syn-3**). The absorption spectra were collected from CH_2Cl_2 solutions

(Figure 3). The absorption maxima of *anti-2*, *anti-3*, and *anti-1* emerged at 662, 710, and 762 nm, respectively. In combination

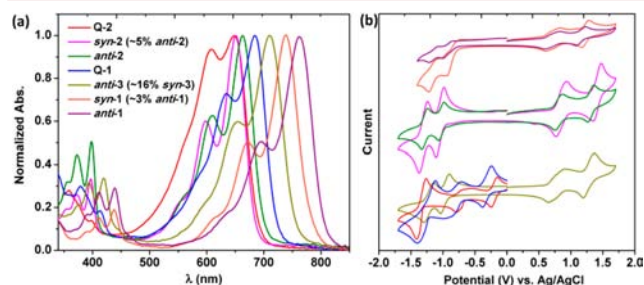


Figure 3. (a) Normalized absorption spectra recorded in CH_2Cl_2 at 1.0×10^{-5} M. (b) Cyclic voltammograms of *syn-1* (with ~3% *anti-1*, top, orange), *anti-1* (top, purple), *syn-2* (with ~5% *anti-2*, middle, magenta), *anti-2* (middle, green), *anti-3* (with ~16% *syn-3*, bottom, yellow), *Q-1* (bottom, blue), and *Q-2* (bottom, red).

with the absorption of previously studied **4H-TAHDI** ($\lambda_{\text{max}} = 778$ nm), a clear trend was illustrated. Namely, as the electron-donating ability of contained heteroatoms increased in the order of $\text{O} < \text{S} < \text{N}(\text{H})$, increasingly red-shifted absorptions were manifested. Moreover, the *anti*-isomers exhibited longer absorption wavelengths than their respective *syn*-isomers ($\lambda_{\text{max}} = 738$ nm for *syn-1* and 651 nm for *syn-2*), and quinoidal molecules displayed blue-shifted absorptions relative to their dihydro- analogues ($\lambda_{\text{max}} = 684$ nm for *Q-1* and 647 nm for *Q-2*). The emission maxima of these compounds occurred in a very similar order with their absorption maxima (Figure S1 and Table 1).

Table 1. Optical and Electronic Properties^a

	λ_{max}^b [nm]	ϵ^c [$\text{L}\cdot\text{mol}^{-1}\cdot\text{cm}^{-1}$]	λ_{em}^d [nm]	LUMO ^e [eV]	HOMO [eV]	E_g [eV]
<i>syn-1</i>	738	6.0×10^4	761	−3.61	−4.97 ^e	1.36 ^f
<i>anti-1</i>	762	3.8×10^4	792	−3.67	−4.98 ^e	1.31 ^f
<i>syn-2</i>	651	5.1×10^4	675	−3.41	−5.17 ^e	1.76 ^f
<i>anti-2</i>	662	3.6×10^4	691	−3.42	−5.12 ^e	1.70 ^f
<i>anti-3</i>	710	4.0×10^4	740	−3.48	−5.03 ^e	1.55 ^f
<i>Q-1</i>	684	6.6×10^4	731	−4.14	−5.84 ^g	1.70 ^h
<i>Q-2</i>	647	5.8×10^4	688	−4.26	−6.02 ^g	1.76 ^h

^aSamples of *syn-1*, *syn-2*, and *anti-3* contained small amounts of their regioisomers (*syn-1* with ~3% *anti-1*, *syn-2* with ~5% *anti-2*, and *anti-3* with ~16% *syn-3*). ^bAbsorption maxima in CH_2Cl_2 . ^cMolar extinction coefficient at λ_{max} . ^dEmission maxima in CH_2Cl_2 . ^eFrom the onset of the first reduction or oxidation waves in CV. ^fBand gap from $(E_{\text{LUMO}} - E_{\text{HOMO}})$. ^gEstimated from the LUMO level and optical band gap E_g . ^hBand gap from the absorption onset.

The electrochemical properties were also examined. Molecules *syn-1*, *anti-1*, *syn-2*, *anti-2*, and *anti-3* all manifested two reversible oxidation and two reversible reduction waves (Figure 3b), with LUMO levels varied from −3.41 to −3.67 eV and HOMO levels from −4.97 to −5.17 eV (Table 1). Oxygen-containing isomers of **2** exhibited a higher LUMO and a lower HOMO than their S-containing counterparts of **1**, consistent with their much larger band gaps. Quinoidal compounds *Q-1* and *Q-2* displayed three reversible reduction waves, with the first one shown at −0.31 and −0.19 V (vs Ag/AgCl) respectively, which echoed their facile chemical reductions. Such low LUMO levels suggested their potential application as

electron-transporting molecules. The oxidation waves for *Q-1* and *Q-2* were not obtainable.

DFT calculations helped further assess the frontier orbitals of the molecules. As depicted in Figure 4, *anti-1* and *syn-1* had

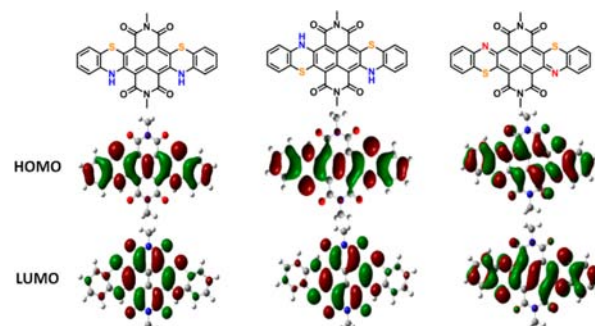


Figure 4. DFT calculated frontier orbitals of *syn-1*, *anti-1*, and *Q-1*.

similar frontier orbital characteristics with previously studied **4H-TAHDI**. With HOMOs distributed over the heterocyclic hexacene framework, LUMOs were nonetheless mainly contributed by the NDI moiety and four heteroatoms. On the other hand, the quinonoid compound *Q-1* displayed a more effectively delocalized HOMO and LUMO over the entire polycyclic scaffold, which is in principle favorable for intermolecular charge transport.¹⁸ Similar frontier orbital geometries were demonstrated by *syn-2*, *anti-2*, and *Q-2* (Figure S6) with their respective analogues. Calculated HOMOs and LUMOs also showed that the orbital coefficients on the heteroatoms shrank evidently from S, N to O, revealing their decreasing contributions in that order.¹⁹

In conclusion, a number of new heterocyclic hexacene diimides containing N, O, and S heteroatoms were synthesized. Particularly, a couple of stable quinoidal heterocycle molecules with low LUMOs were acquired. Specifically, while *anti*- and *syn*-isomers were obtained as mixtures from synthetic reactions, only the *anti*-precursors could be dehydrogenated to afford the quinoidal structures. Moreover, this further transformation of *anti*-isomers allowed isolation of the *syn*-isomers, whereas pure *anti*-isomers were attained by reducing the quinoidal oxidation products. The identities of the heteroatoms sensitively influenced the frontier orbital energy levels and the optical properties of the molecules. The highly delocalized, low LUMO levels of the quinoidal structures show promise for potential n-type semiconductor applications.

■ ASSOCIATED CONTENT

Supporting Information

Experimental procedures and analytical data. This material is available free of charge via the Internet at <http://pubs.acs.org>.

■ AUTHOR INFORMATION

Corresponding Author

*E-mail: dhzhao@pku.edu.cn.

Notes

The authors declare no competing financial interest.

■ ACKNOWLEDGMENTS

We acknowledge the financial support of the National Natural Science Foundation of China (Projects 21174004 and 21222403).

■ REFERENCES

- (1) (a) Bhosale, S. V.; Jani, C. H.; Langford, S. J. *Chem. Soc. Rev.* **2008**, *37*, 331–342. (b) Sakai, N.; Mareda, J.; Vauthey, E.; Matile, S. *Chem. Commun.* **2010**, 46, 4225–4237. (c) Bhosale, S. V.; Bhosale, S. V.; Bhargava, S. K. *Org. Biomol. Chem.* **2012**, *10*, 6455–6468.
- (2) (a) Gao, X.; Di, C.; Hu, Y.; Yang, X.; Fan, H.; Zhang, F.; Liu, Y.; Li, H.; Zhu, D. *J. Am. Chem. Soc.* **2010**, *132*, 3697–3699. (b) Sakai, N.; Matile, S. *J. Am. Chem. Soc.* **2011**, *133*, 18542–18545. (c) Hwang, D. K.; Dasari, R. R.; Fenoll, M.; Alain-Rizzo, V.; Dindar, A.; Shim, J. W.; Deb, N.; Fuentes-Hernandez, C.; Barlow, S.; Bucknall, D. G.; Audebert, P.; Marder, S. R.; Kippelen, B. *Adv. Mater.* **2012**, *24*, 4445–4450. (d) Zhao, Y.; Domoto, Y.; Orentas, E.; Beuchat, C.; Emery, D.; Mareda, J.; Sakai, N.; Matile, S. *Angew. Chem., Int. Ed.* **2013**, *125*, 9940–9943. (e) Schneebeli, S. T.; Frasconi, M.; Liu, Z.; Wu, Y.; Gardner, D. M.; Strutt, N. L.; Cheng, C.; Carmieli, R.; Wasielewski, M. R.; Stoddart, J. F. *Angew. Chem., Int. Ed.* **2013**, *49*, 13100–13104. (f) He, T.; Stolte, M.; Würthner, F. *Adv. Mater.* **2013**, *48*, 6951–6955. (g) Smith, A. R.; Iverson, B. L. *J. Am. Chem. Soc.* **2013**, *135*, 12783.
- (3) Thalacker, C.; Röger, C.; Würthner, F. *J. Org. Chem.* **2006**, *71*, 8098–8105.
- (4) (a) Gao, X.; Qiu, W.; Yang, X.; Liu, Y.; Wang, Y.; Zhang, H.; Qi, T.; Liu, Y.; Lu, K.; Du, C.; Shuai, Z.; Yu, G.; Zhu, D. *Org. Lett.* **2007**, *9*, 3917–3920. (b) Röger, C.; Würthner, F. *J. Org. Chem.* **2007**, *72*, 8070–8075.
- (5) Katsuta, S.; Tanaka, K.; Maruya, Y.; Mori, S.; Masuo, S.; Okujima, T.; Uno, H.; Nakayama, K. I.; Yamada, H. *Chem. Commun.* **2011**, 47, 10112–10114.
- (6) (a) Hu, Y.; Gao, X.; Di, C.; Yang, X.; Zhang, F.; Liu, Y.; Li, H.; Zhu, D. *Chem. Mater.* **2011**, *23*, 1204–1215. (b) Ye, Q.; Chang, J.; Huang, K.-W.; Chi, C. *Org. Lett.* **2011**, *22*, 5960–5963. (c) Fukutomi, Y.; Nakano, M.; Hu, J.-Y.; Osaka, I.; Takimiy, K. *J. Am. Chem. Soc.* **2013**, *135*, 11445–11448. (d) Gao, J.; Li, Yan; Wang, Z. *Org. Lett.* **2013**, *15*, 1366–1369.
- (7) (a) Suraru, S.-L.; Zschieschang, U.; Klauk, H.; Würthner, F. *Chem. Commun.* **2011**, 47, 11504–11506. (b) Suraru, S.-L.; Burschka, C.; Würthner, F. *J. Org. Chem.* **2014**, *79*, 128–139.
- (8) Chen, X.; Guo, Y.; Tan, L.; Yang, G.; Li, Y.; Zhang, G.; Liu, Z.; Xu, W.; Zhang, D. *J. Mater. Chem. C* **2013**, *1*, 1087–1092.
- (9) Yue, W.; Gao, J.; Li, Y.; Jiang, W.; Di Motta, S.; Negri, F.; Wang, Z. *J. Am. Chem. Soc.* **2011**, *133*, 18054–18057.
- (10) (a) Bhosale, S. V.; Jani, C. H.; Lalander, C. H.; Langford, S. J. *Chem. Commun.* **2010**, 46, 973–975. (b) Bhosale, S. V.; Jani, C. H.; Lalander, C. H.; Langford, S. J.; Nerush, I.; Shapter, G. J.; Villamaina, D.; Vauthey, E. *Chem. Commun.* **2011**, 47, 8226–8228. (c) Bhosale, S. V.; Adsul, M.; Shitre, G. V.; Bobe, S. R.; Bhosale, S. V.; Privér, S. H. *Chem.—Eur. J.* **2013**, *19*, 7310–7313. (d) Bhosale, S. V.; Kobaisi, M. A.; Bhosale, R. S.; Bhosale, S. V. *RSC Adv.* **2013**, *3*, 19840–19843.
- (11) (a) Langhals, H.; Kinzel, S. *J. Org. Chem.* **2010**, *75*, 7781–7784. (b) Tan, L.; Guo, Y.; Yang, Y.; Zhang, G.; Zhang, D.; Yu, G.; Xu, W.; Liu, Y. *Chem. Sci.* **2012**, *3*, 2530–2541. (c) Li, C.; Xiao, C.; Li, Y.; Wang, Z. *Org. Lett.* **2013**, *15*, 682–685. (d) Ye, Q.; Chang, J.; Huang, K. W.; Shi, X.; Wu, J.; Chi, C. *Org. Lett.* **2013**, *15*, 1194–21197.
- (12) (a) Cai, K.; Yan, Q.; Zhao, D. *Chem. Sci.* **2012**, *3*, 3175–3182. (b) Cai, K.; Xie, J.; Zhao, D. *J. Am. Chem. Soc.* **2014**, *136*, 28–31.
- (13) (a) Fin, A.; Petkova, I.; Doval, D. A.; Sakai, N.; Vauthey, E.; Matile, S. *Org. Biomol. Chem.* **2011**, *9*, 8246–8252. (b) Zhu, X.; Tsuji, H.; Nakabayashi, K.; Ohkashim, S.; Nakamara, E. *J. Am. Chem. Soc.* **2011**, *133*, 16342–16345. (c) Li, Y.; Heng, W. K.; Lee, B. S.; Aratani, N.; Zafra, J. L.; Bao, N.; Lee, R.; Sung, Y. M.; Shu, Z.; Huang, K.-W.; Webster, R. D.; Navarrete, J. T. L.; Kim, D.; Osuka, A.; Casado, J.; Ding, J.; Wu, J. *J. Am. Chem. Soc.* **2012**, *134*, 14913–14922. (d) Sun, Z.; Wu, J. *J. Mater. Chem.* **2012**, *22*, 4151–4160. (e) Shimizu, A.; Kishi, R.; Nakano, M.; Shiomi, D.; Sato, K.; Takui, T.; Hisaki, I.; Miyata, M.; Tobe, Y. *Angew. Chem., Int. Ed.* **2013**, *23*, 6076–6079.
- (14) Di, C.; Li, J.; Yu, G.; Xiao, Y.; Guo, Y.; Liu, Y.; Qian, X.; Zhu, D. *Org. Lett.* **2008**, *10*, 3025–3028.
- (15) The ^1H NMR chemical shifts of *anti*-**1** and *syn*-**1** were observed to change slightly with solution concentration, suggesting the occurrence of intermolecular aggregation in CDCl_3 solution.
- (16) Suraru, S.-L.; Würthner, F. *J. Org. Chem.* **2013**, *78*, S227–S238.
- (17) In ref 11c the synthesis of **1** in DMF was reported, but the major product *syn*-**1** was misassigned to *anti*-**1**.
- (18) Yamaguchi, Y.; Ogawa, K.; Nakayama, K.; Ohba, Y.; Katagiri, H. *J. Am. Chem. Soc.* **2013**, *135*, 19095–19098.
- (19) Appleton, A. L.; Brombosz, S. M.; Barlow, S.; Sears, J. S.; Bredas, J. L.; Marder, S. R.; Bunz, U. H. F. *Nat. Commun.* **2010**, *1*, 91–96.